ISSN 1674-1056
http://cpb.iphy.ac.cn
http://iopscience.iop.org/cpb
中国物理 B
Chinese Physics
中国物理
Chinese Physics B

Birefringence via Doppler broadening and prevention of information hacking

Humayun Khan, Muhammad Haneef, Bakhtawar
Citation: Chin. Phys. B . 2018, 27(1): 014201. **doi:** 10.1088/1674-1056/27/1/014201

Journal homepage: http://cpb.iphy.ac.cn; http://iopscience.iop.org/cpb

What follows is a list of articles you may be interested in

Electro-optical properties of high birefringence liquid crystal compounds with isothiocyanate and naphthyl group

Zeng-Hui Peng(彭增辉), Qi-Dong Wang(王启东), Shao-Xin Wang(王少鑫), Li-Shuang Yao(姚丽双), Yong-Gang Liu(刘永刚), Li-Fa Hu(胡立发), Zhao-Liang Cao(曹召良), Quan-Quan Mu(穆全全), Cheng-Liang Yang(杨程亮), Li Xuan(宣丽)
Chin. Phys. B . 2017, 26(9): 094210. **doi:** 10.1088/1674-1056/26/9/094210

Modulation instabilities in randomly birefringent two-mode optical fibers

Jin-Hua Li(李金花), Hai-Dong Ren(任海东), Shi-Xin Pei(裴世鑫), Zhao-Lou Cao(曹兆楼), Feng-Lin Xian(咸冯林)
Chin. Phys. B . 2016, 25(12): 124208. **doi:** 10.1088/1674-1056/25/12/124208

Coupled thermal-optic effects and electrical modulation mechanism of birefringence crystal with Gaussian laser incidence

Zhou Ji, He Zhi-Hong, Ma Yu, Dong Shi-Kui
Chin. Phys. B . 2015, 24(9): 094203. **doi:** 10.1088/1674-1056/24/9/094203

Drift effect on vacuum birefringence in a strong electric and magnetic field

Huang Yong-Sheng, Wang Nai-Yan, Tang Xiu-Zhang
Chin. Phys. B . 2015, 24(3): 034201. **doi:** 10.1088/1674-1056/24/3/034201

Designing of a polarization beam splitter for the wavelength of1310 nm on dual-core photonic crystal fiber with high birefringence and double-zero dispersion

Bao Ya-Jie, Li Shu-Guang, Zhang Wan, An Guo-Wen, Fan Zhen-Kai
Chin. Phys. B . 2014, 23(10): 104218. **doi:** 10.1088/1674-1056/23/10/104218

Birefringence via Doppler broadening and prevention of information hacking

Humayun Khan, Muhammad Haneef†, and Bakhtawar

Laborotary of Theoretical Physics, Department of Physics, Hazara University Mansehra, KP, Pakistan

(Received 3 August 2017; revised manuscript received 12 September 2017; published online 17 November 2017)

We propose a new scheme for the coherent control of birefringent light pulses propagation in a four-level atomic medium. We modify the splitting of a light pulse by controlling the electric and magnetic responses. The Doppler broadening effect is also noted on the propagation of the birefringent pulses. The dispersions of the birefringence beams are oppositely manipulated for delay and advancement of time at a Doppler width of 10γ. A time gap is created between the birefringence beams, which protects from hacking of information. The time gap is then closed to restore the pulse into the original form by a reverse manipulation of the dispersion of the birefringence beams, i.e., introducing another medium whose transfer function is the complex conjugate of that of the original medium. The results are useful for secure communication technology.

Keywords: birefringence, Doppler broadening, time gap, hacking

PACS: 42.25.Lc, 42.25.Kb, 42.50.–p **DOI:** 10.1088/1674-1056/27/1/014201

1. Introduction

Over the years, the field of light matter interaction, which can best be described by quantum optics at the quantum mechanical level, has been a hot topic of research.[1–5] The phenomenon of negative refractive index in atomic systems achieved by the interaction of atoms with suitable electric and magnetic components of the laser field has received considerable attention.[6,7] Impressive efforts have been made to investigate propagation of light through a chiral medium, which splits the light beam into birefringent left/right circular polarized beams with different refractive indices.[8] One of the refractive indices has gone by increasing the delays of the beam, while the decrease in the other indices advances the beam.[9–11] McCall[12] in 2011 used the concept of splitting of a light beam into an accelerated leading part and a decelerated trailing part in the creation of a temporal time gap. A few years ago, following the concept of space time duality, a research group demonstrated the first experimental cloak.[13]

The natural birefringent materials exhibit a double image.[14–17] Birefringence has numerous applications. It is used in optical devices, such as liquid crystal displays, light modulators, color filters, and wave plates. It plays an important role in the second harmonic generation and also many other nonlinear processes.[18–20] The process of manipulating the speed of light in such a way that a time gap is created in it is called temporal or event cloaking. An event occurring in the time gap is cloaked (hidden) from the detectors. The time gap is then closed so that a specific observer could receive the information of light in its original form. The ability to hide events opens a number of new exciting possibilities in quantum optics.[21–23]

A large number of research articles have been published to control light pulse via Doppler broadening in atomic configurations.[24–26] In this article, we theoretically investigate the birefringence of a light beam in a chiral medium by using the Doppler broadening configuration and spectral hole burning regions. One of the circularly polarized beams is slowed down and the other is speeded up in the medium. The left/right circularly polarized beams delay and advance with the control field. This creates a temporal time gap and hacking can be controlled due to which information can be hidden. We also use the transfer function and phase shift theorem to enhance the temporal time gap. Our present article is a significant step toward the development of noised free secure communication technology between various channels and also reduces the hacking process. Our results show the importance of birefringence to improve the hacking technology.

2. Model and its dynamics

We choose a four-level double V-type atomic configuration of the cesium medium. The energy level diagram of the atom field interaction is shown in Fig. 1. This system has two degenerate excited states $|3\rangle$ & $|4\rangle$, a ground state $|1\rangle$, and a meta stable state $|2\rangle$, which are subjected to the selection rules. The upper excited levels $|3\rangle$ and $|4\rangle$ are coupled with the ground level $|1\rangle$ by the superposition of two probe fields having Rabi frequencies $G_{\rm p}$. The two probes vary by phase φ and have the same detuning $\Delta_{\rm p}$. The excited levels $|3\rangle$ and $|4\rangle$ are coupled with the meta stable state $|2\rangle$ by two control fields having Rabi frequencies $G_{1,2}$. The ground state $|1\rangle$ is coupled with the meta stable state $|2\rangle$ by a magnetic field of Rabi fre-

†Corresponding author. E-mail: haneef.theoretician@gmail.com

© 2018 Chinese Physical Society and IOP Publishing Ltd

quency $G_{\rm m}$ having detuning $\Delta_{\rm m}$. The decayed $\gamma_{i=1,2,3,4,5}$ are shown in the figure. To derive the equations of motion and study the optical response of the chiral medium, we proceed with the following self Hamiltonian (H_0) and interaction picture Hamiltonian ($H_{\rm I}$) in the dipole and rotating wave approximations:

$$\begin{aligned} H_0 &= \hbar\omega_1 |1\rangle\langle 1| + \hbar\omega_2 |2\rangle\langle 2| + \hbar\omega_3 |3\rangle\langle 3| + \hbar\omega_4 |4\rangle\langle 4|, \\ H_{\rm I} &= \Big[-\frac{\hbar}{2} G_{\rm p} \mathrm{e}^{-\mathrm{i}\Delta_{\rm p} t} |1\rangle\langle 4| - \frac{\hbar}{2} G_{\rm p} \mathrm{e}^{\mathrm{i}\varphi} \mathrm{e}^{-\mathrm{i}\Delta_{\rm p} t} |1\rangle\langle 3| \\ &\quad - \frac{\hbar}{2} G_{\rm m} \mathrm{e}^{-\mathrm{i}\Delta_{\rm m} t} |1\rangle\langle 2| - \frac{\hbar}{2} G_1 \mathrm{e}^{-\mathrm{i}\Delta_1 t} |2\rangle\langle 4| \\ &\quad - \frac{\hbar}{2} G_2 \mathrm{e}^{-\mathrm{i}\Delta_2 t} |2\rangle\langle 3| \Big] + \text{H.c.} \end{aligned}$$

The master equation which is used for the dynamics of the system is written as

$$\dot{\rho} = -\frac{\mathrm{i}}{\hbar}[H_{\rm I}, \rho] - \sum \frac{1}{2}\gamma_{ij}(R^{\dagger} R\rho + \rho R^{\dagger} R - 2R\rho R^{\dagger}), \quad (1)$$

where $R^{\dagger}$ and R are the raising/lowering operators, γ_{ij} represent the decay rates, and ρ is the density matrix. By using the master Eq. (1) for the dynamics of the system, the three important coupling rates equations are obtained as

$$\begin{aligned} \dot{\tilde{\rho}}_{12}^{(1)} &= A_1 \tilde{\rho}_{12}^{(1)} + \frac{\mathrm{i}}{2} G_{\rm m} (\tilde{\rho}_{11}^{(0)} - \tilde{\rho}_{22}^{(0)}) + \frac{\mathrm{i}}{2} G_1^{*} \tilde{\rho}_{14}^{(1)} \\ &\quad + \frac{\mathrm{i}}{2} G_2^{*} \tilde{\rho}_{13}^{(1)} - \frac{\mathrm{i}}{2} G_{\rm p} \tilde{\rho}_{32}^{(0)} - \frac{\mathrm{i}}{2} G_{\rm p} \mathrm{e}^{\mathrm{i}\varphi} \tilde{\rho}_{42}^{(0)}, \quad (2) \\ \dot{\tilde{\rho}}_{13}^{(1)} &= A_2 \tilde{\rho}_{13}^{(1)} + \frac{\mathrm{i}}{2} G_{\rm p} (\tilde{\rho}_{11}^{(0)} - \tilde{\rho}_{33}^{(0)}) + \frac{\mathrm{i}}{2} G_2 \tilde{\rho}_{12}^{(1)} \\ &\quad - \frac{\mathrm{i}}{2} G_{\rm p} \mathrm{e}^{\mathrm{i}\varphi} \tilde{\rho}_{43}^{(0)} - \frac{\mathrm{i}}{2} G_{\rm m} \tilde{\rho}_{33}^{(0)}, \quad (3) \\ \dot{\tilde{\rho}}_{14}^{(1)} &= A_2 \tilde{\rho}_{14}^{(1)} + \frac{\mathrm{i}}{2} G_{\rm p} \mathrm{e}^{\mathrm{i}\varphi} (\tilde{\rho}_{11}^{(0)} - \tilde{\rho}_{44}^{(0)}) + \frac{\mathrm{i}}{2} G_1 \tilde{\rho}_{12}^{(1)} \\ &\quad - \frac{\mathrm{i}}{2} G_{\rm p} \tilde{\rho}_{34}^{(0)} - \frac{\mathrm{i}}{2} G_{\rm m} \tilde{\rho}_{24}^{(0)}. \quad (4) \end{aligned}$$

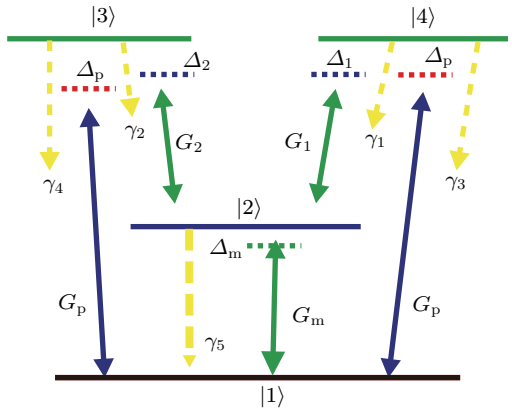


Fig. 1. (color online) Energy diagram of the four-level atomic system.

The atoms are initially prepared in the ground state $|1\rangle$. The population of atoms primarily in the other states are assumed to be zero. Therefore, $\tilde{\rho}_{11}^{(0)} = 1$ while $\tilde{\rho}_{22,33,42,32,43,34,34}^{(0)} = 0$. To evaluate the system density dynamics of $\tilde{\rho}_{13}^{(1)}$, $\tilde{\rho}_{14}^{(1)}$, and $\tilde{\rho}_{12}^{(1)}$ in its steady state condition, we use the following expression:

$$\boldsymbol{Q}(t) = \int_{-\infty}^{t} \mathrm{e}^{-M(t-t')} B \mathrm{d}t = -M^{-1} B, \quad (5)$$

where $\boldsymbol{Q}$ is a column matrix of the coupled density, $\boldsymbol{B}$ is the column matrix of constants, and $\boldsymbol{M}$ is a 3×3 matrix. The solution is in the form

$$\tilde{\rho}_{13}^{(1)} + \tilde{\rho}_{14}^{(1)} = G_{\rm p}\beta_{EE} + G_{\rm m}\beta_{EB}, \quad (6)$$

$$\tilde{\rho}_{12}^{(1)} = G_{\rm m}\beta_{BB} + G_{\rm p}\beta_{BE}, \quad (7)$$

where β_{EE} and β_{BB} are electric and magnetic polarizibalities, while β_{EB} and β_{BE} are related to the chiral coefficients. The electric polarization is defined as $P_{\rm e} = N(\sigma_{13}\tilde{\rho}_{13}^{(1)} + \sigma_{14}\tilde{\rho}_{14}^{(1)})$, whereas $\sigma_{13} \cong \sigma_{14} = \sigma$. Here σ_{13} and σ_{14} are the electric dipole moments. The magnetization can be obtained from equation $M = N\mu_{12}\tilde{\rho}_{12}^{(1)}$, where μ_{12} is the magnetic dipole moment, and N is the total number of atoms (atomic density). Putting $G_{\rm p} = \sigma E/\hbar$ and $G_{\rm m} = \mu_{12}B/\hbar$, with $B = \mu_0(M+H)$, we obtain the electric polarization and magnetization. The electric and magnetic polarizations are in the form of chiral coefficients, while the electric and magnetic susceptibilities are defined as $P_{\rm e} = \varepsilon_0\chi_{\rm e}^{(1)}E + \xi_{EH}H/c$ and $M = \chi_{\rm m}^{(1)}H + \frac{\xi_{HE}H}{\mu_0 c}E$. Comparing the above two polarizations and magnetizations, we obtain the first-order complex electric and magnetic susceptibilities as well as the chiral coefficients for this atomic system, which are written as

$$\chi_{\rm e}^{(1)} = \frac{\beta_{EE} + \mu_0(\beta_{EB}\beta_{BE} - \beta_{BB}\beta_{EE})}{\varepsilon_0(1-\mu_0\beta_{BB})}, \quad (8)$$

$$\chi_{\rm m}^{(1)} = \frac{\mu_0\beta_{BB}}{1-\mu_0\beta_{BB}}, \quad (9)$$

$$\xi_{EH}^{(1)} = \frac{c\mu_0\beta_{EB}}{1-\mu_0\beta_{BB}}, \quad (10)$$

$$\xi_{HE}^{(1)} = \frac{c\mu_0\beta_{\rm BE}}{1-\mu_0\beta_{BB}}, \quad (11)$$

where

$$\beta_{BE} = \frac{N\sigma\mu_{12}B_1}{P\hbar}, \quad (12)$$

$$\beta_{EB} = \frac{N\sigma\mu_{12}(G_1[\exp(-\mathrm{i}\theta_1) + G_2[\exp(-\mathrm{i}\theta_2)])}{P\hbar}, \quad (13)$$

$$\beta_{EE} = \frac{N\sigma^2(B_2+B_3)}{2A_2P\hbar}, \quad (14)$$

$$\beta_{BB} = \frac{2\mathrm{i}N\mu_{12}^2A_2}{P\hbar}, \quad (15)$$

$$A_1 = \mathrm{i}\Delta_{\rm m} - \frac{(\gamma_1+\gamma_2+\gamma_3+\gamma_4+\gamma_5)}{2}, \quad (16)$$

$$A_2 = \mathrm{i}\Delta_{\rm p} - \frac{(\gamma_3+\gamma_4+\gamma_5)}{2}, \quad (17)$$

$$P = 4A_1A_2(G_1^2+G_2^2), \quad (18)$$

$$B_1 = G_1\mathrm{e}^{\mathrm{i}(\varphi+\theta_1)} + G_2\mathrm{e}^{\mathrm{i}\theta_2}, \quad (19)$$

$$B_2 = 4\mathrm{i}A_1A_2 + \mathrm{i}G_1^2 - \mathrm{i}G_1G_2\,\mathrm{e}^{\mathrm{i}(\varphi+\theta_1-\theta_2)}, \tag{20}$$

$$B_3 = \mathrm{i}(4A_1A_2 + G_2^2)\,\mathrm{e}^{\mathrm{i}\varphi} - \mathrm{i}G_1G_2\,\mathrm{e}^{\mathrm{i}(\theta_1-\theta_2)}. \tag{21}$$

To introduce the Doppler broadening effect in the medium, we replace $\Delta_\mathrm{p} = \Delta_\mathrm{p} + k_\mathrm{m}v$ and $\Delta_\mathrm{m} = \Delta_\mathrm{m} + \eta_\mathrm{m}k_\mathrm{p}v$, where $k_\mathrm{p} = 2\pi/\lambda_\mathrm{p}$ and $k_\mathrm{m} = 2\pi/\lambda_\mathrm{m}$. If the magnetic field co-propagates to the electric probe then $\eta_\mathrm{m} = -1$ and if counter-propagates then $\eta_\mathrm{m} = 1$. For simplification, we plug here $k_\mathrm{p,m} = k$. With the above conditions, we obtain the velocity dependent susceptibility and chiral coefficients $\chi_\mathrm{e}^{(1)}(kv)$, $\chi_\mathrm{m}^{(1)}(kv)$, $\xi_{EH}^{(1)}(kv)$, and $\xi_{HE}^{(1)}(kv)$. The Doppler susceptibilities and chiral coefficients are the average over the Maxwellian distribution and given as

$$\chi_\mathrm{e} = \frac{1}{V_\mathrm{D}\sqrt{\pi}}\int_{-\infty}^{\infty}\chi_\mathrm{e}(kv)\,\mathrm{e}^{-\frac{(kv)^2}{V_\mathrm{D}^2}}\,\mathrm{d}(kv), \tag{22}$$

$$\chi_\mathrm{m} = \frac{1}{V_\mathrm{D}\sqrt{\pi}}\int_{-\infty}^{\infty}\chi_\mathrm{m}(kv)\,\mathrm{e}^{-\frac{(kv)^2}{V_\mathrm{D}^2}}\,\mathrm{d}(kv), \tag{23}$$

$$\xi_{EH} = \frac{1}{V_\mathrm{D}\sqrt{\pi}}\int_{-\infty}^{\infty}\xi_{EH}(kv)\,\mathrm{e}^{-\frac{(kv)^2}{V_\mathrm{D}^2}}\,\mathrm{d}(kv), \tag{24}$$

$$\xi_{HE} = \frac{1}{V_\mathrm{D}\sqrt{\pi}}\int_{-\infty}^{\infty}\xi_{HE}(kv)\,\mathrm{e}^{-\frac{(kv)^2}{V_\mathrm{D}^2}}\,\mathrm{d}(kv), \tag{25}$$

where V_D is the Doppler width and depends upon the absolute temperature. Its value is written as

$$V_\mathrm{D} = \sqrt{K_\mathrm{B}T_\mathrm{a}\omega^2/Mc^2}, \tag{26}$$

where K_B is the Boltzman constant, T_a is the absolute temperature, M is the molecular mass, and c is the speed of light in a vacuum. When the light ray enters into the chiral medium, it becomes birefringent. The divided rays have left and right circular polarizations with refractive indices $n_\mathrm{r}^{(-)}$ and $n_\mathrm{r}^{(+)}$, respectively. One refractive index slightly decreases while the other slightly increases. The refractive index is given as

$$n_\mathrm{r}^{(\pm)} = \mathrm{Re}\left[\sqrt{\varepsilon_\mathrm{r}\mu_\mathrm{r} - \frac{(\xi_{EH}+\xi_{HE})^2}{4}} \pm \mathrm{i}\,\frac{(\xi_{EH}-\xi_{HE})}{2}\right], \tag{27}$$

where $\varepsilon_\mathrm{r} = (1+\chi_\mathrm{e})$ and $\mu_\mathrm{r} = 1+\chi_\mathrm{m}$. The complex phase velocity is written as $v_\mathrm{p}^{\pm} = c/n_\mathrm{r}^{(\pm)}$. The real and imaginary parts of the complex velocity are related to the propagation speed in the medium and the damping speed, respectively. When the light beams propagate in a vacuum, all the waves have the same speed c, but when the light beams are propagating in a chiral dispersive medium, the waves propagate with a complex group speed $v_\mathrm{g}^{\pm} = c/N_\mathrm{g}^{\pm}$. The waves pulse has a complex group index of refraction. The complex group index $N_\mathrm{g}^{(\pm)}$ of the pulse is written as

$$n_\mathrm{g}^{(\pm)} = n_\mathrm{r}^{(\pm)} + \omega_\mathrm{p}\frac{\partial n_\mathrm{r}^{(\pm)}}{\partial\Delta_\mathrm{p}}. \tag{28}$$

This index of refraction has real and imaginary parts related to the group velocity and the damping group index, respectively, where ω_p is the frequency of the probe field. The complex group divergence between the two pulses is

$$\theta_\mathrm{g}^\mathrm{D} = \frac{\pi L}{\lambda}(n_\mathrm{g}^{(+)} - n_\mathrm{g}^{(-)}). \tag{29}$$

The complex group velocity is written as $v_\mathrm{g}^{\pm} = c/n_\mathrm{g}^{(\pm)}$.

$$E_\mathrm{i}(t) = \frac{1}{\sqrt{2\pi}}\int_{-\infty}^{\infty}E_\mathrm{i}(\Delta_\mathrm{p})\,\mathrm{e}^{-\mathrm{i}\Delta_\mathrm{p}t}\,\mathrm{d}\Delta_\mathrm{p}, \tag{30}$$

where $\Delta_\mathrm{p} = \omega_\mathrm{p} - \omega_0$ for our proposed system. This wave packet in the frequency domain is considered as

$$E_\mathrm{i}(\Delta_\mathrm{p}) = \frac{1}{\sqrt{\tau_0}}\,\mathrm{e}^{-\frac{\tau_0^2\Delta_\mathrm{p}^2}{4}}, \tag{31}$$

where τ_0 is the input pulse width. In a chiral medium, the pulse splits into left/right circular polarized light beams. The beams have different transit times in a chiral medium due to the slight difference in the refractive indices.

The transmission frequency spectrum $E_\mathrm{tr}(\Delta_\mathrm{p})$ of the incident event $E_\mathrm{i}(\Delta_\mathrm{p})$ is then equal to the product

$$E_\mathrm{tr}^{(+)}(\omega_\mathrm{p}) = E_\mathrm{i}(\Delta_\mathrm{p})H_1^{(+)}(\Delta_\mathrm{p}), \tag{32}$$

$$E_\mathrm{tr}^{(-)}(\Delta_\mathrm{p}) = E_\mathrm{i}(\Delta)H_1^{(-)}(\Delta_\mathrm{p}), \tag{33}$$

where $H_1^{(+)}(\Delta_\mathrm{p})$ and $H_1^{(-)}(\Delta_\mathrm{p})$ are the transfer functions of the medium for left and right circular polarized beams

$$H_1^{(+)}(\Delta_\mathrm{p}) = \mathrm{e}^{\mathrm{i}\Delta_\mathrm{p}t^{(+)}}, \tag{34}$$

$$H_1^{(-)}(\Delta_\mathrm{p}) = \mathrm{e}^{\mathrm{i}\Delta_\mathrm{p}t^{(-)}}. \tag{35}$$

The transmission spectrum in the time domain is written as

$$E_\mathrm{tr}(t) = F^{-1}[E_\mathrm{i}(\Delta_\mathrm{p})H_1^{(\pm)}(\Delta_\mathrm{p})], \tag{36}$$

where $t^{\pm} = L/v_\mathrm{g}^{\pm}$. The time gap is created between the intervals $t_0 + t^{(+)}$ and $t_0 + t^{(-)}$, whose width is equal to $t^{(+)} - t^{(-)}$. If an external event $E_\mathrm{ext}(t)$ interacts with $E_\mathrm{tr}(t)$ in this gap, then $E_\mathrm{ext}(t)E_\mathrm{tr}(t) = 0$. The transmitted wave packet experiences no effect of the interacting event that occurs inside this gap. The information of the wave packet is not hacked in the gap and it will transmit without being detected until the gap is closed. For the specific observer to receive the original information of the incident wave packet, the gap is closed by reverse manipulation. In this case, another medium whose transfer function is the complex conjugate of the original medium is required, i.e.,

$$H_2^{(+)}(\Delta_\mathrm{p}) = [H_1^{(+)}(\Delta_\mathrm{p})]^*, \tag{37}$$

$$H_2^{(-)}(\Delta_\mathrm{p}) = [H_1^{(-)}(\Delta_\mathrm{p})]^*. \tag{38}$$

The output transmission frequency spectrum of $E_\mathrm{i}(\Delta_\mathrm{p})$ is then written as

$$E_\mathrm{out}(\Delta_\mathrm{p}) = E_\mathrm{tr}(\Delta_\mathrm{p})H_2(\Delta_\mathrm{p}) = E_\mathrm{i}(\Delta_\mathrm{p}). \tag{39}$$

The output signal in the time domain is obtained by taking the inverse Fourier transform of $g_{\rm out}(\omega_{\rm p})$ as

$$E_{\rm out}(t) = F^{-1}[E_{\rm out}(\Delta_{\rm p})] = E_{\rm i}(t). \tag{40}$$

The output signal is obtained in its original form.

3. Results and discussion

The propagation of a light pulse through a four-level chiral atomic system is under consideration in this article. We use atomic units in this work. A scaling parameter γ is taken, $\gamma = 10$ MHz, and all parameters are scaled to γ. The dipole moments are supposed according to the Einstein coefficient as $\sigma = \sqrt{\frac{3\hbar\lambda^3(\gamma_2+\gamma_3)/2}{8\pi^2}}$ and $\mu_{12} = c\sqrt{\frac{3\hbar\lambda^3\gamma_5}{8\pi^2}}$. The plots are traced for the electric and magnetic susceptibilities and chiral coefficients. The refractive index and divergence angle are modified due to the additional terms of the chiral coefficients. When light enters to the chiral medium, it splits the light ray into left and right circular polarization beams. Our main interest is to study the Doppler broadening effect on the complex refractive index, which is related to the divergence angle between the two rays. The Doppler broadening effect changes the optical properties of a chiral medium. In this medium, the splitting of the ray into left and right circular polarizations varies with the Doppler broadening.

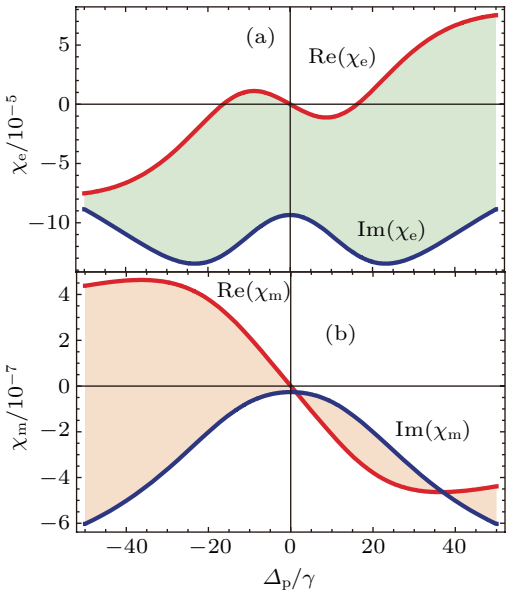


Fig. 2. (color online) Real and imaginary parts of the electric and magnetic susceptibilities vs. $\Delta_{\rm p}/\gamma$, where $\gamma_{1,2,3,4} = 1\gamma$, $\gamma_5 = 0.001\gamma$, $G_{1,2} = 20\gamma$, $V_{\rm D} = 5\gamma$, $\Delta_{1,\rm m} = 0\gamma$, $\varphi = 0$, $\theta_{1,2} = \pi/2$, $\eta_{\rm m} = 1$, and $\lambda = 586$ nm.

Figure 2 shows the variation of the real and imaginary parts of the electric and magnetic susceptibilities with the probe de-tuning $\Delta_{\rm p}/\gamma$. The real part of susceptibility is related to the dispersion spectrum and the imaginary part is related to the absorption spectrum of the probe field. The magnetic responses are very small as compared to the electric responses and large contribution to the optical properties is made by the electric responses.

Figure 3 shows the real and imaginary parts of chiral coefficients ξ_{EH} and ξ_{HE}. The sum of real and imaginary parts of the chiral coefficients vanishes as $\mathrm{Re}(\xi_{HE}) + \mathrm{Re}(\xi_{EH}) = 0$ and $\mathrm{Im}(\xi_{HE}) + \mathrm{Im}(\xi_{EH}) = 0$. The difference of the real and imaginary parts of the chiral coefficients ($\mathrm{Re}(\xi_{HE}) - \mathrm{Re}(\xi_{EH}) \neq 0$ and $\mathrm{Im}(\xi_{\rm HE}) - \mathrm{Im}(\xi_{EH}) \neq 0$) contributes to the complex refractive index and the related optical properties such as the complex divergence angle between the left/right circular polarized beams.

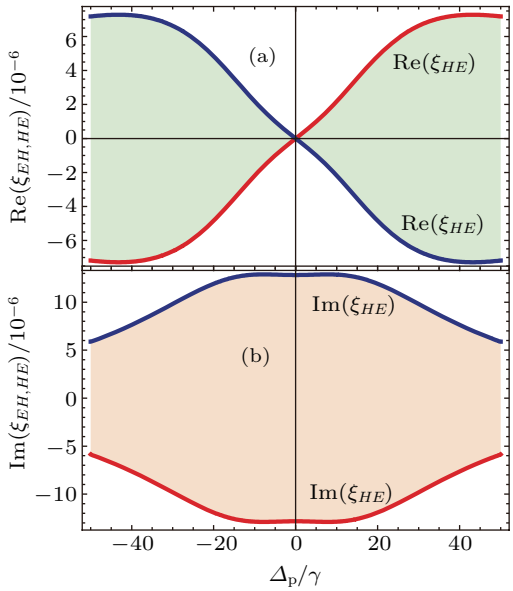


Fig. 3. (color online) Real and imaginary parts of the chiral coefficients vs. $\Delta_{\rm p}/\gamma$ with the same parameters given in Fig. 2

Figure 4 shows the variation of the phase refractive indices with the probe detuning and Doppler width. The phase refractive indices $n_{\rm r}^{\pm}$ of the birefringent beams have slight change $\Delta n = (n_{\rm r}^{(+)}) - (n_{\rm r}^{(-)})$, which shows the divergence of the beam and different transit time in the medium. The phase refractive indices of the birefringence beams have reverse manipulation with Doppler width in Fig. 4(b). This shows the creation of a time gap for information hiding to reduce hacking.

Figure 5 shows the group refractive indices and divergence angle between the birefringent pulses with Doppler width. The Doppler width is temperature dependent. The group indices show a reverse variation with Doppler width and finally become saturated. Initially $n_{\rm g}^{+}$ increases in the positive domain and creates a delay time in the medium, $n_{\rm g}^{-}$ decreases and becomes negative which creates advances in time. This opens a time gap for reducing hacking of information. Finally both refractive indices become saturated with Doppler width and the time gap remains constant.

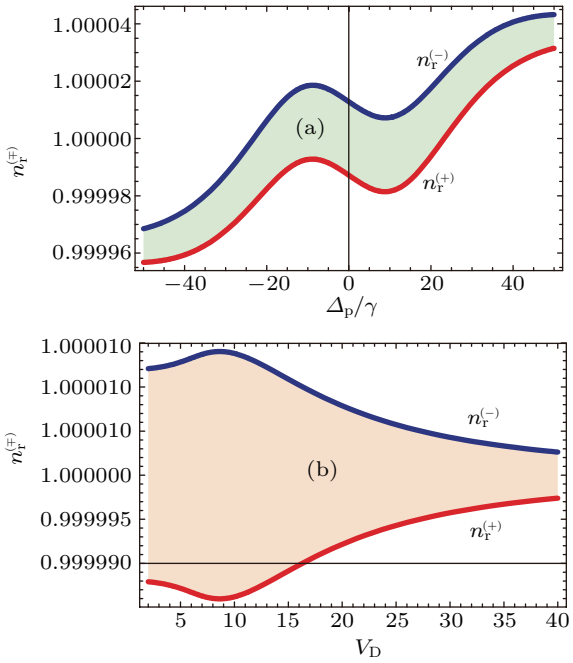


Fig. 4. (color online) (a) Refractive index vs. Δ_p/γ with the parameters in Fig. 2; (b) refractive index vs. V_D with the same parameters and $\Delta_p = 0\gamma$.

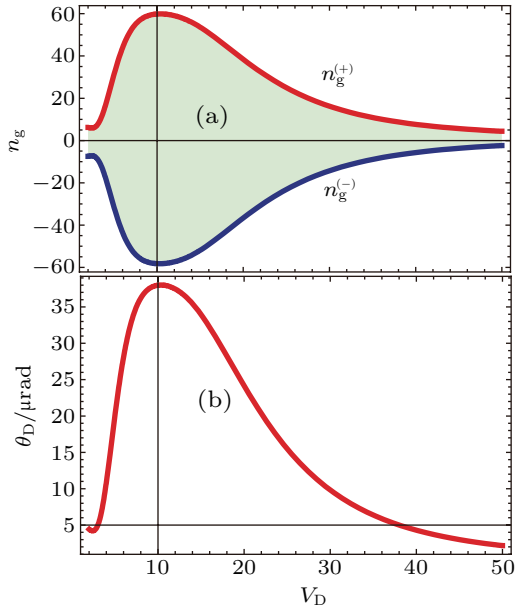


Fig. 5. (color online) (a) Group index and (b) divergence angle vs. V_D with the same parameters of Fig. 2 but $\Delta_p = 20\gamma$ and $\omega_p = 1000\gamma$.

Figure 6 shows the input pulse intensity, transition pulse intensity, and output pulse intensity of the birefringence beams vs. t/τ_0. The input pulse width τ_0 is supposed to be 2.8 ns. The input pulse intensity has a Gaussian form as shown in Fig. 6(a). The transmission pulse intensities of the birefringence beams are also Gaussian. In this case, the pulse of the left circular polarized beam advances and the right circular polarized beam delays within the chiral medium at the Doppler width $V_D = 10\gamma$. This delay and advancement of time in birefringence creates a times gap about the central time t_0 where the pulse amplitude is zero. In the time gap, information is not detectable and no one can hack the information of the carrier pulse. This time gap reduces the hacking of information as shown in Fig. 6(b). Finally, the birefringence beam is restored to the original form by the reverse manipulation of dispersion. For this, another medium whose transfer function is the complex conjugate of that of the original medium is needed. This medium will delay the left circular polarized beam and advance the right circular polarized beam. Under this condition, the time gap between the birefringence beams is closed and the output pulse is obtained in the original input form and the information is now detectable as shown in Fig. 6(c).

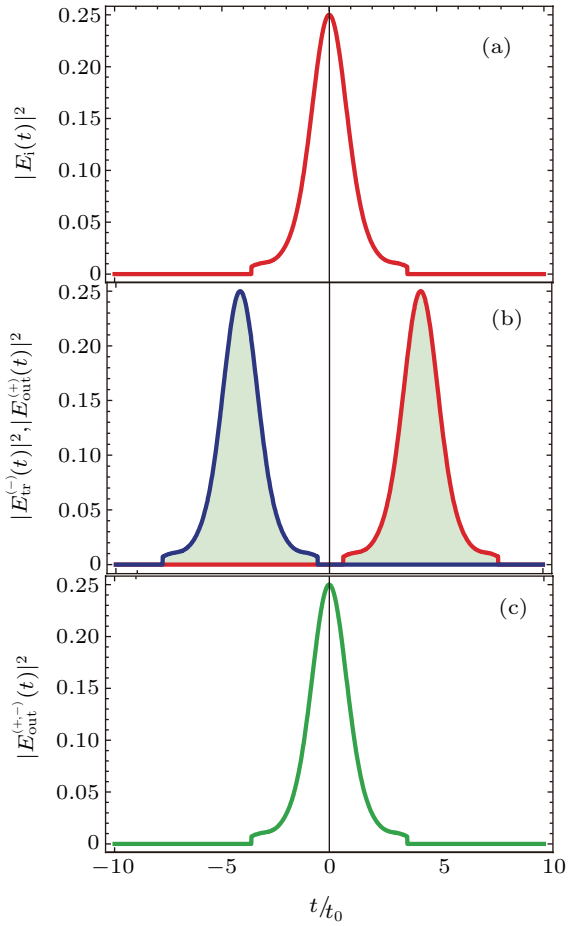


Fig. 6. (color online) (a) Input pulse intensity, (b) transmission intensity of birefringence, (c) output intensity of birefringence beams vs. t/τ_0 with the same parameters of Fig. 2 but $V_D = 10\gamma$, $\Delta_p = 20\gamma$, and $\tau_0 = 2.8$ ns.

4. Conclusion

We used a four-level atomic medium to measured both electric and magnetic responses for birefringence. In this atomic system, we applied an electric and magnetic probe and two control fields. We introduced the Doppler broadening effect in this atomic system and measured the variation in propagating beams in the medium. We observed splitting of light beams into left/right circular polarized beams. We measured the differences in phase and group refractive indices. Since

information is carried by the pulse, therefore we measured the group indices for left/right circular polarized beams. These beams show different transit time in the medium due to the difference in the group indices. The difference in transit time creates a time gap where the pulse amplitude is zero and the information is not detectable in the time gap. This reduces the hacking possibility of information in communication systems. The time gap is then closed to restore the pulse into the original form by a reverse manipulation of the dispersion of the birefringence beams. Our results show potential applications in secure communication technology.

References

[1] Loudon R 2000 *The Quantum Theory of Light* (3rd Edn.) (Oxford: Oxford University Press)

[2] Humayun K and Haneef M 2017 *Canadian Journal of Physics* (Accepted)

[3] Bacha B A, Ghafor F, Ahmad I and Rahman A 2014 *Laser physics* **24** 055401

[4] Hong X M, Wan S B, Hong W L and Chun C 2016 *Chin. Phys. B* **25** 080309

[5] Jin H L, Hai D R, Shi X P, Zhao L C and Feng L X 2016 *Chin. Phys. B* **25** 124208

[6] Thommen Q and Mandel P 2006 *Phys. Rev. Lett.* **96** 053601

[7] Orth P P, Henning R, Keitel C H and Evers J 2013 *New. J. Phys.* **15** 1

[8] Humayun K and Haneef M 2017 *Laser Phys.* **27** 055201

[9] Kastel J, Fleischhauer M, Susanne, Yelin F and Walsworth R L 2007 *Phys. Rev. lett.* **99** 073602

[10] Ghosh A and Fischer P 2006 *Phys. Rev. Lett.* **97** 173002

[11] Jaggard D L, Mickelson A R and Papas C H 1979 *Appl. Phys.* **18** 211

[12] McCall M W, Favaro A, Kinsler P and Boardman A 2011 *J. Opt.* **13** 024003

[13] Fridman M, Farsi A, Okawachi Y and Gaeta A L 2012 *Nature* **481** 62

[14] Leonhardt U 2006 *Science* **312** 1777

[15] Service R F and Cho A 2010 *Science* **330** 1622

[16] Pendry J B, Schurig D and Smith D R 2006 *Science* **312** 1780

[17] Shalaev V M 2008 *Science* **322** 384

[18] Born, Max and Wolf E 1999 *Principles of Optics: Electromagnetic Theory of Propagation, Interference and Diffraction of Light* (7th Edn.) (Cambridge: Cambridge University Press)

[19] Elert and Glenn 2007 *The Physics Hypertextbook* (Refraction hypertextbook.com)

[20] Sharma and Kailash K 2006 *Optics: Principles and Applications* (Burlington: Academic Press)

[21] McCall M 2013 *Contemp. Phys.* **54** 273

[22] Kasapi A, Jain M, Yin G Y and Harris S E 1995 *Phys. Rev. Lett.* **74** 2447

[23] Jabar M S A, Bacha B A and Ahmad I 2016 *Chin. Phys. B* **25** 084205

[24] Kash M M and Scully 1999 *Phys. Rev. Lett.* **82** 5229

[25] Agarwal G S and Dey T N 2003 *Phys. Rev. A* **68** 063816

[26] Kuang S, Du P and Gang R 2008 *Opt. Express* **16** 11604